Journal of Cultural Heritage 25 (2017) 101–112

Available online at
ScienceDirect
www.sciencedirect.com

Elsevier Masson France
EM|consulte
www.em-consulte.com/en

Original article

AFM and SIMS surface and cation profile investigation of archaeological obsidians: New data

Nick Laskaris[a], Ioannis Liritzis[b,*], Massimo Bonini[c], Francesca Ridi[c], Reinhard Kersting[d], Fahad Al-Otaibi[e]

[a] Laboratory of Applied Mechanics and Acoustics, Department of Sound and Musical, Instruments Technology, Technological Educational Institute of Ionian Islands, Lixouri, 28200 Cephallonia, Greece
[b] King Saud University, Saudi Arabia and Laboratory of Archaeometry, Department of Mediterranean Studies, University of the Aegean, 85100 Rhodes, Greece
[c] University of Florence, Department of Chemistry "Ugo Schiff" and CSGI, via della Lastruccia 3, 50019 Sesto Fiorentino (FI), Italy
[d] TASCON GmbH, Heisenbergstrasse 15, 48149 Muenster, Germany
[e] King Saud University, Department of History, Saudi Arabia

ARTICLE INFO

Article history:
Received 24 September 2016
Accepted 30 November 2016
Available online 3 January 2017

Keywords:
Obsidian
AFM
SIMS
TOF-SIMS
Surface roughness
Rind
SIMS-SS dating
Cation profiling
Hydration

ABSTRACT

Obsidian surface roughness and rind structure both play a major influence on the Obsidian Hydration Dating (OHD). AFM (Atomic Force Microscopy) investigation coupled with quadrupole SIMS hydrogen data profiles establish a validation criterion of quantitative evaluation of roughness for OHD dating purposes. More evidence of the importance of the surface morphology at the nanoscale is given for five obsidian tools of different origin. The latter relates to the dynamic ion influx diffusion kinetics between surface and surrounded sediment media, and the obsidian structure, thus, 2D and 3D surface mapping, as well as, cation profiling (H, C, Mg, Al, F, S, Cl, CN, O isotopes) were made by TOF-SIMS and quad-SIMS. It was found that the C and Mg are considered as imposed criteria for accepting suitability of H^+ profiles for further processing by SIMS-Surface Saturation dating method. The effect of roughness to dating is discussed.

1. Introduction

Obsidian is a natural glass that undergoes hydration because of environmental humidity and forms a hydration rim in its interface layer (few microns below the surface). It is known that the hydration of obsidian is a complicated, diffusion-limited phenomenon, which is strongly affected mainly by environmental factors of temperature, water concentration on the glass surface, as well as, pristine water (glass structural water) [1–4].

In the last decade, novel approaches to the investigation of the obsidian surfaces by means of Scanning Electron Microscopy (SEM) and Secondary Ion Mass Spectroscopy (SIMS) have revealed the influence of microlithic inclusions on the hydration process [5–7]. Furthermore, preliminary results from investigation of the surface with Atomic Force Microscopy (AFM) have shown that the surface roughness has a significant impact on SIMS measurement [6–9]. Roughness derives from various causes, the weathering (burial conditions), cleavage during carving of the tool, usage.

Here, new measurements of AFM along with quadrupole SIMS and ToF-SIMS mapping and cation profiling on obsidians had lead to further assessment and evaluation of the criterion for choosing and accepting suitable obsidian surface areas for SIMS, and cation profiles. Investigations on surface roughness and profile data scatter and dispersion prior to any H^+ SIMS profile for SIMS-SS dating purposes [5] has been instrumentally and statistically documented.

2. AFM on archaeological materials and obsidians

Since its discovery [10], thanks to its versatility, the AFM technique has been widely used in many different fields, such as biology and micro/nano-electronics. Although there are studies reporting its use in modern glasses (especially for the study of optical fibers), there are very few reports describing its use in archeological glasses.

Considering the most relevant studies reporting the use of AFM in ancient obsidians and manufactured glasses these are by:

* Corresponding author.
E-mail address: liritzis@rhodes.aegean.gr (I. Liritzis).

http://dx.doi.org/10.1016/j.culher.2016.11.014

Schmitz et al. in 1995 [11]; Schreiner et al. in 1999 [12] showing the characterization of the surface of mediaeval vitro (stained glass) exposed to natural environmental conditions; Carmona et al. in 2010 [13], comparing the surface micro-structures in ancient and modern glasses degraded by chemicals, Zacharias et al., 2010 [14] on the authenticity of glazed pottery; Melcher et al. in 2010 [15] studying the degradation of glass artifacts. AFM has been previously used in the investigation of obsidians by Liritzis et al. in 2008 [8,9] and by Novak and Stevenson in 2012 [16]. These results pointed out that the surface roughness can potentially influence the sputtering of ions, the diffusion profiles of cations into the glass and especially distorts the concentration of water (as H^+) versus depth.

3. SIMS on surfaces: the effect of roughness

The SIMS method is based on the sputtering of secondary ions from the surface of a material that is bombarded by a primary ion beam [17]. The type and the quantity of the sputtered secondary ions from the surface provide useful information on the chemical composition of the surface under examination. By using a profilometer to measure the total depth of the crater formed by the bombardment, information on the concentration distribution of the elements versus depth can be inferred. Several studies on materials, mainly in the research field of micro-/nano-electronics (e.g. thin films of silicon or germanium), show that the measurement of a surface by SIMS is subjected to the influence of the roughness of the surface [18].

Irrespective to the material's composition and the nature of the ion beam, the influence of the roughness on the experimental output (chemical composition versus depth profile) is twofold: the first one is connected to the intrinsic roughness of the material; the second one concerns the additional roughness induced by the ion bombardment [16–20]. In fact, the two types of impact in processed surfaces of silica was found for primer ion beam of oxygen (O) [19,21], and in the same surface but for primer ion beam of cesium (Cs) [20].

The impact of surface morphology on SIMS results has been comprehensively discussed [18,22], assessing that natural cracks, pinholes or swellings could lead to unreliable results. The surface roughness has an influence on the spread of secondary ions during the bombardment and, as a result, distorted data for the composition of the surface are recorded as they reach the mass spectrometer. In addition, the roughness induced by the ion beam further influences the distribution of the secondary ions. In a recent report, Novak and Stevenson [16] have investigated modern and archaeological obsidian surfaces by means of SIMS and AFM, concluding that the roughness measured by SIMS is larger than its real value. It is not yet clear at which depth this induced roughness starts to be generated, while this information would be important to give a correct interpretation of the hydrogen profiles. In 2008 the first results from the AFM measurements were published [8,9] and they reveal that there seems a correlation between the spread of the profile concentration values found by SIMS and the value of the roughness obtained by AFM. This correlation could be related to the effect of the surface roughness on the dispersion of the secondary ions and the collection of disturbed data from the mass spectrometer.

This paper aims at confirming and expanding the validity of this approach, evaluating the importance of the structural characterization at the micro- and nanoscale, by complimentary quad-SIMS and ToF-SIMS mapping and cation profiling of rinds on obsidians of different archaeological origin.

4. Experimental details

All samples were investigated by means of a Park XE-100 AFM in contact mode (NSC36 probes, radius of curvature < 10 nm). To avoid microscopic cracks and inhomogeneities, the regions to be scanned by AFM were chosen with the aid of an optical microscope [8].

Secondary ion mass spectrometry (SIMS) analyses were conducted at the commercial laboratory of Evans Analytical Group, East Windsor, NJ, USA, and the profiles were collected using PHI Model 6300 and 6600 quadrupole-based secondary ion mass spectrometers. A 5.0 KeV Cs^+ primary ion beam with an impact angle of 60° with respect to surface normal was used and negative secondary ions were detected. The measurements were performed using a 300×300 micron ion beam raster, which results in very little visual disruption to the sample surface. Generally, the SIMS depth scale accuracy for archaeological samples is within 5–10%. This translates into an estimated error of ± 0.05 μm. This value is not equivalent to the ± 0.01–0.03 μm standard deviation usually associated with SIMS because of the irregular surface topography present on naturally cleaved samples. For polished test samples crater depths are measured using a Dektak 6 M stylus profilometer which is reproducible to within 1% on flat, well-controlled samples [8].

ToF-SIMS measurements were carried out within the scope of an ION-TOF ToF-SIMS.5-200 demonstration in the laboratories of Tascon in Germany. The chosen analytical conditions were adapted to the respective analytical needs. General information about ToF-SIMS instrumentation, modes of operation and typical applications can be found elsewhere [23].

A representative image displaying one of the AFM experiments is reported for each sample, showing the positioning of the tip over the surface. Table 1 reports the analyzed samples together with their place of origin. These together with some more measured by TOF-SIMS were chosen to investigate surface differences under different environments (Aegean, Carpathian, Asia Minor, Continental Greece), some of them have had stereo microscopic images with differences in surface appearance, while others are compared to samples from same stratigraphy and age of earlier made SIMS profiles.

5. Measurements by AFM and SIMS

5.1. AFM

5.1.1. Sample RHO-4 (ULUCAK)

Optical microscopy results show that the sample is not flat and that it is not homogeneous in the micrometric scale. The sample features cracks, voids and inhomogeneities typically in the range of few microns. The percentage of the area covered by such features is lower than 10%. The vast majority of the surface consists of regions similar to the one shown in the micrograph in Table 1. In these regions the surface mainly consists of sub-micrometric spheroidal structures. The size and shape of these objects are quite homogeneous. Typically, particle diameter is in the range between 20 nm and 100 nm, while the height is typically below 10 nm (Fig. 1).

5.1.2. Sample RHO-8 (ULUCAK)

Optical microscopy investigation (see Table 1) reveals a microscopic structure partly similar that of RHO-4, while AFM results display significant differences. Rod-like crystallites are present on top of spheroidal structures similar to those observed in RHO-4 (see Fig. 2). The dimensions of rod-like particles are typically around 100 nm in cross-section and few hundreds of nm in length.

5.1.3. Sample RHO-363 (MORAVANY-3)

By naked eye this sample looks very different from the others; in fact, the sample is not as black colored as the others, and is partly translucent. The surface is extremely flat, except for some linear scratches, clearly visible in the optical micrograph (see Table 1).

Table 1
Provenance and visual aspect of obsidian samples analyzed with AFM.

Sample n°	Provenance	Macrophoto	Micrograph
RHO-4 (ULUCAK)	Smyrna Neolithic settlement Minor Asia		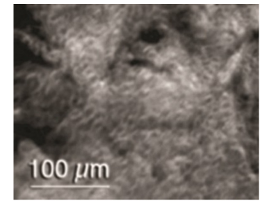
RHO-8 (ULUCAK)	Smyrna Neolithic settlement Minor Asia		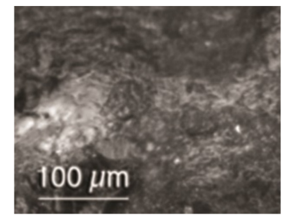
RHO-363 (MORAVANY-3)	Moravany site Early Neolithic settlement East Slovakia		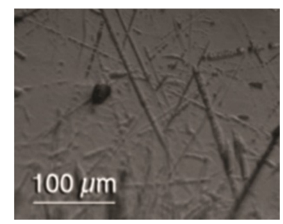
RHO-442 (YAL-2)	Island of Gyali Neolithic settlement Dodecanese, Greece		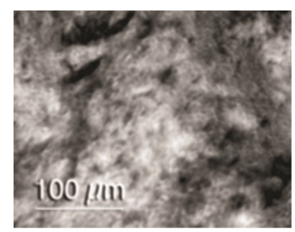
RHO-450 (YR-2)	Island of Youra “Cyclops Cave” settlement Late palaeolithic layer Alonissos, Greece		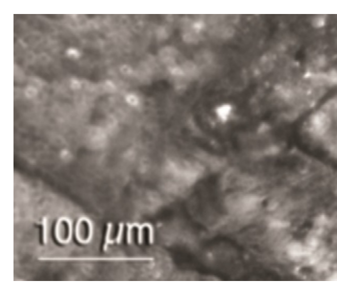

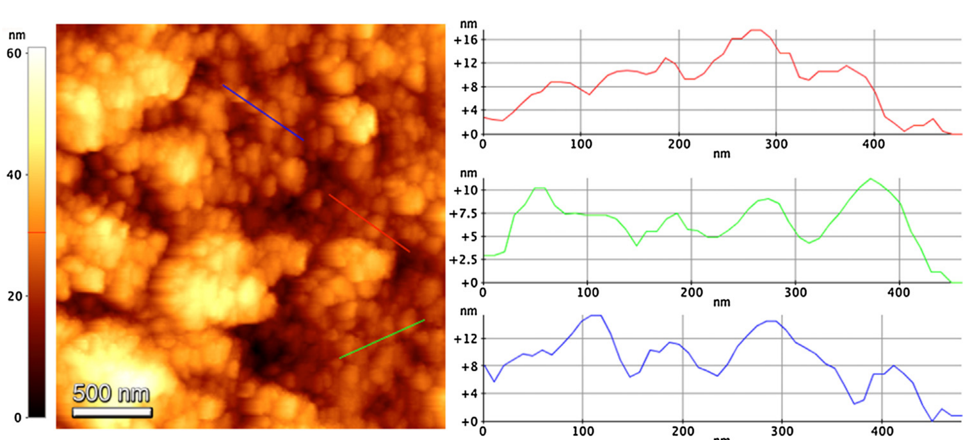

Fig. 1. AFM image of the sample RHO-4 (ULUCAK). The height profiles along three lines are shown. The surface mainly consists of nanometric spheroidal structures.

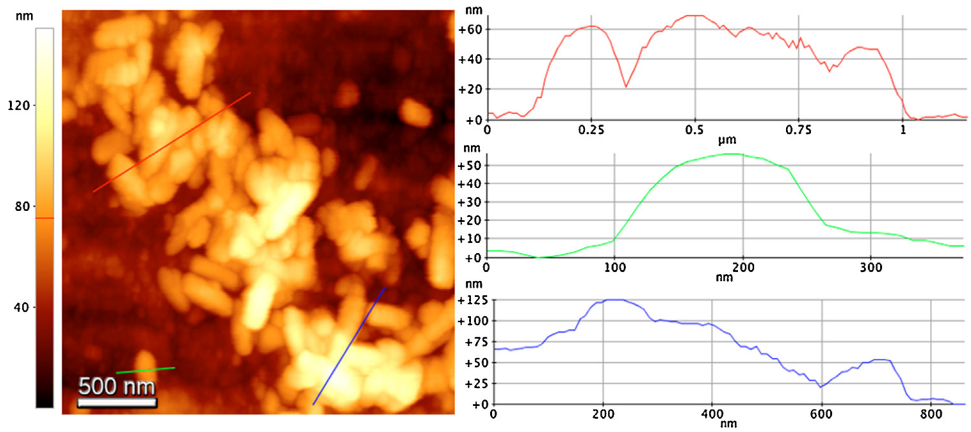

Fig. 2. AFM image of the sample RHO-8 (ULUCAK). The height profiles along three lines are shown. The surface consists of rod-like nanometric particles on top of spheroidal structures.

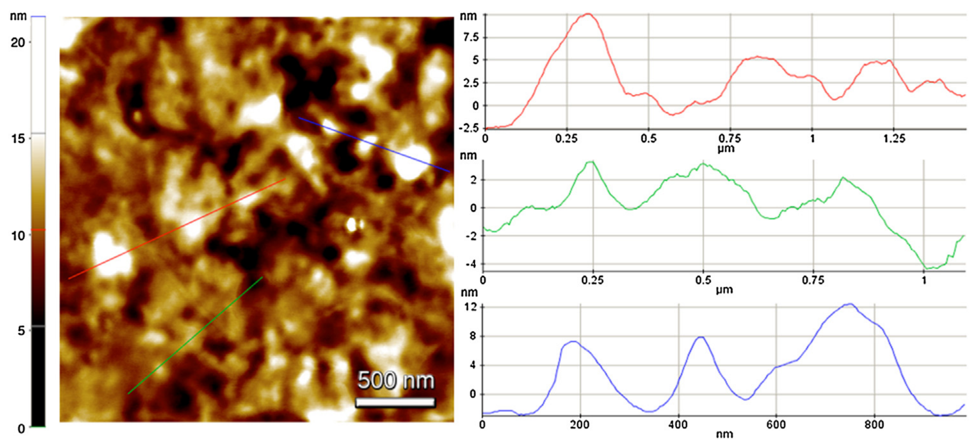

Fig. 3. AFM image of the sample RHO-363 (MORAVANY-3). The height profiles along three lines are reported.

AFM results reveal the presence in the flat regions of inhomogeneities whose height is typically below 10 nm (see Fig. 3).

5.1.4. *Sample RHO-442 (YAL-2)*

Optical microscopy (see Table 1) shows that sample RHO-442 (YAL) on the microscopic scale is very similar to sample RHO-4 (ULUCAK), featuring cracks and inhomogeneities, typically in the range of few microns. Again, the majority of the surface consists of regions similar to the one where the AFM probe is placed in Fig. 4. At the nanoscale, AFM shows the presence of crystallites and inhomogeneities, irregular both in size and shape. Small particles with diameter of few tens of nanometers are also present.

5.1.5. *Sample RHO-450 (YR-2)*

At the microscopic scale, the surface of this sample is quite homogeneous (see micrograph in Table 1). AFM investigation shows the presence at the nanoscale of globular structures whose size is roughly 10 nm in height and few hundreds of nanometers in diameter (see Fig. 5).

Table 2 summarizes the values of roughness for each sample. Values were obtained by means of AFM as an average over 4 different regions, each one having an area of 25 μm^2. The roughness is reported as the arithmetic average, R_a calculated as:

$$R_a = \frac{1}{n}\sum_{i=1}^{n}|y_i|$$

Where y_i represents the height of a single AFM pixel.

Table 2
Roughness coefficient values R_a for obsidians of Table 1.

Sample	R_a (nm)
RHO-4	14 ± 4
RHO-8	35 ± 8
MORAVANY-3	9 ± 3
YAL-2	42 ± 22
YR-2	23 ± 15

5.2. *SIMS profiles and SIMS-SS dating*

A novel dating approach using SIMS-SS to investigate secondary ion mass spectrometry-surface saturation layer has been proposed. The water diffusion into the obsidian follows a S-like curve that obeys satisfactorily enough the 2nd Fick's law of diffusion (Eq. (1)) – a diffused region and an exponential region, both reflect two different diffusion mechanisms [5] (Fig. 6), where *c* is the concentration. A solution of this mathematical expression for certain boundary conditions provides the age equation of diffusion time (Eq. (2)).

Fick's Second Law (for 1D diffusion):

$$\frac{\partial c}{\partial t} = D\frac{\partial^2 c}{\partial x^2} \leftarrow \text{from equation of continuity} \tag{1}$$

Analytical solutions can be found for specific initial and boundary conditions

$$T = \frac{(C_i - C_s)^2\left[\frac{1.128}{1-\frac{0.177kC_i}{C_s}}\right]^2}{4Dseff\left[\left.\frac{dC}{dx}\right|_{x=0}\right]^2} \tag{2}$$

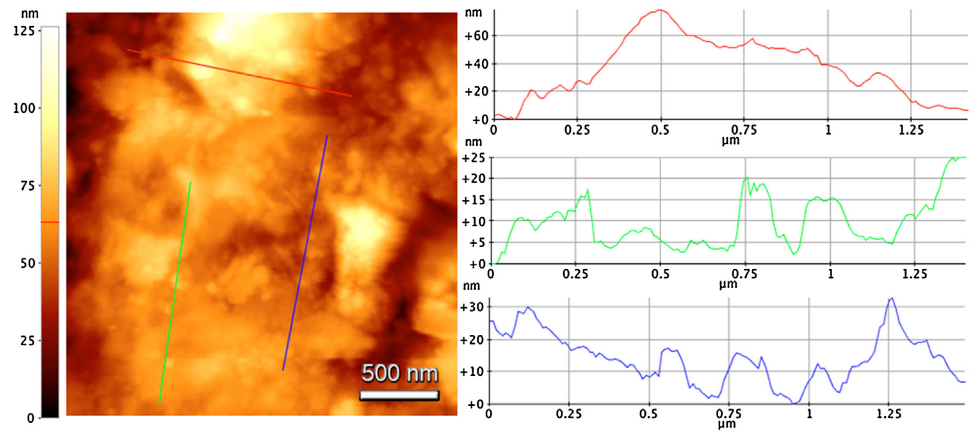

Fig. 4. AFM image of the sample RHO-442 (YAL-2). The height profiles along three lines are shown.

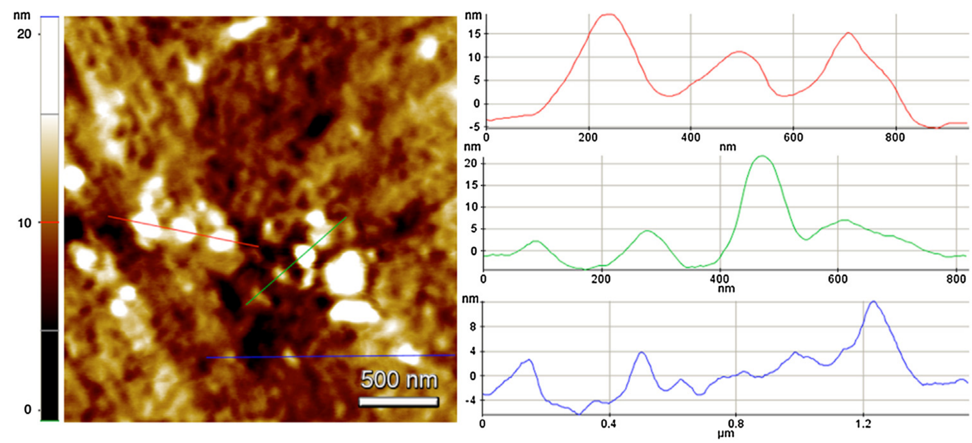

Fig. 5. AFM image of the sample RHO-450 (YR-2). The height profiles along three lines are shown.

Where, *C* the concentration of water for intrinsic (I) and surface saturation (S) layer respectively, *k* a parameter from Crank's basic book (The Mathematics of diffusion 1975, Clarendon Press, Oxford) solutions for non-dimensional plots, and D_{seff} the effective diffusion coefficient [5].

It is based on the modeling of the water distribution into the obsidian surface. The Water distribution is measured with the SIMS method and on the new concept of a Saturation Surface layer (SS). This layer is created on the first 1–3 μm of the obsidian surface due to the different speed of the two diffusion Mechanisms. The first mechanism transfers the ambient water from the environment into the exterior surface of obsidian, and the second mechanism is responsible for the diffusion process into the interior of the artifact (Fig. 6A, B).

However, the determination of the SS layer, i.e. the little flat (plateau) segment in the diffused region of the sigmoid curve, is a crucial age parameter. This SS layer is formed with a highest concentration as a progressive front during the diffusion time defined by *Cs* and *xs*. This is located by, (i) the sliding progressive regressions to determine a near-zero slope, and, (ii) through a repeated derivatives approach starting from the initial points to the whole diffused region. This way an emerged pattern for safe location of SS appears. But the latter has shown cases where the location of SS and/or the polynomial fitting of the profile are both problematic, and uncertain ages are linked to the surface topography.

It has been shown [9] that the proper choice of the spot where SIMS analysis is performed represents a crucial step in the reliability of the proposed dating method. When this condition is properly fulfilled, the accuracy of the results should directly depend on the roughness of the sample. An indication of the correlation between SIMS-diffused profile properties and surface roughness aids selection of appropriate obsidian surfaces for dating. Fig. 6A is a sigmoid profile of obsidian produced by SIMS indicating the diffused region. In the diffused region a linear regression fit ($y = a + bx$) defines the dispersion, which reflects the degree of roughness and sputtering (Fig. 6B). The dispersion is defined by the Standard Deviation of Residuals (Rstd). Thus, Rstd is the standard deviation of residuals between data and linear fitting in diffused region, and R_a, is the arithmetic mean deviation calculated by the AFM. Fig. 7 shows the correlation between Rstd and R_a.

6. Discussion on roughness

In Fig. 7 for the sake of comparison, the newly investigated samples are reported together with those of three pairs of values already published in previous works [8,9]. The results suggest a linear correlation between AFM roughness and SIMS standard deviation (as highlighted by the pink rectangle in Fig. 8) except of RHO-4 and YR-2, which appreciably deviate from the linear trend. At this stage we are not able to explain the behavior of these last two samples. Most probably, it is due to experimental issues such as the statistical representativeness of the areas investigated by AFM and SIMS or the topography of craters formed during SIMS measurements, work that is under way.

It has already been shown elsewhere [8,9] that a correlation exists between the roughness parameters extracted by means of AFM and the Rstd factor obtained by SIMS. The dispersion of SIMS data points is influenced by both the surface roughness of the

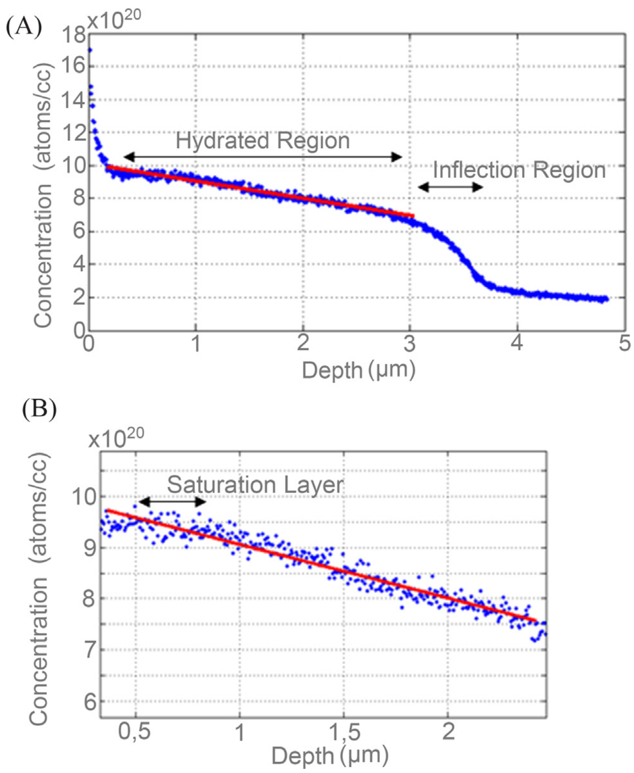

Fig. 6. A. SIMS profile for hydrogen with a best fit applied. It consists of the diffused region (long) and exponential region (right). B. Blow up of diffused region of (A). Note the scatter around the best fit (red) and the segment with arrow the surface saturation (SS) layer.

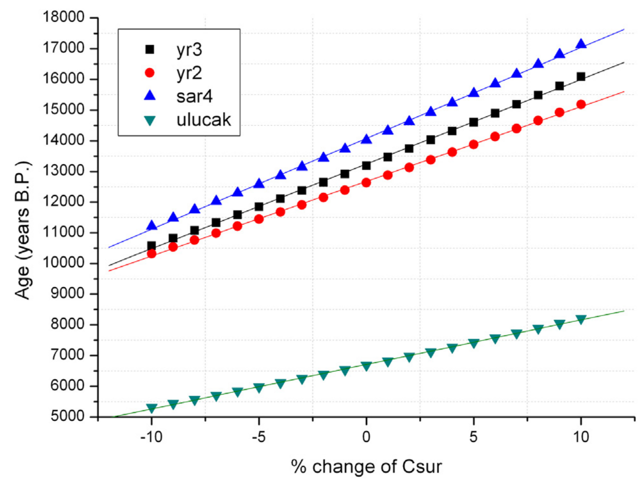

Fig. 8. Change in age for % change of saturation concentration for four samples derived from four different obsidian sources.

sample and the ripple roughness induced by the primary ion beam [19–21]. The latter has already been shown to negatively affect the accuracy of SIMS analyses in [22], also for obsidians in [16], and has been reconfirmed and accurately evaluated by AFM.

Ultimately, the effect of roughness in SIMS-SS dating and especially regarding accuracy in the SS layer estimation is discussed. Figs. 6 and 8 show the effect of the dispersion of scattered data points in the determination of SS layer, on the age obtained for four obsidian tools. A $\pm$10% error in *Cs* of SS layer gives a ~25% error in age. It is apparent that the suppression of roughness by selecting proper raster area for ion beam to get the H^+ profile is very crucial. In obsidian tools the hydration layers can reach thicknesses up to 15–20 µm, while this layer does not exceed 1.5–2 µm

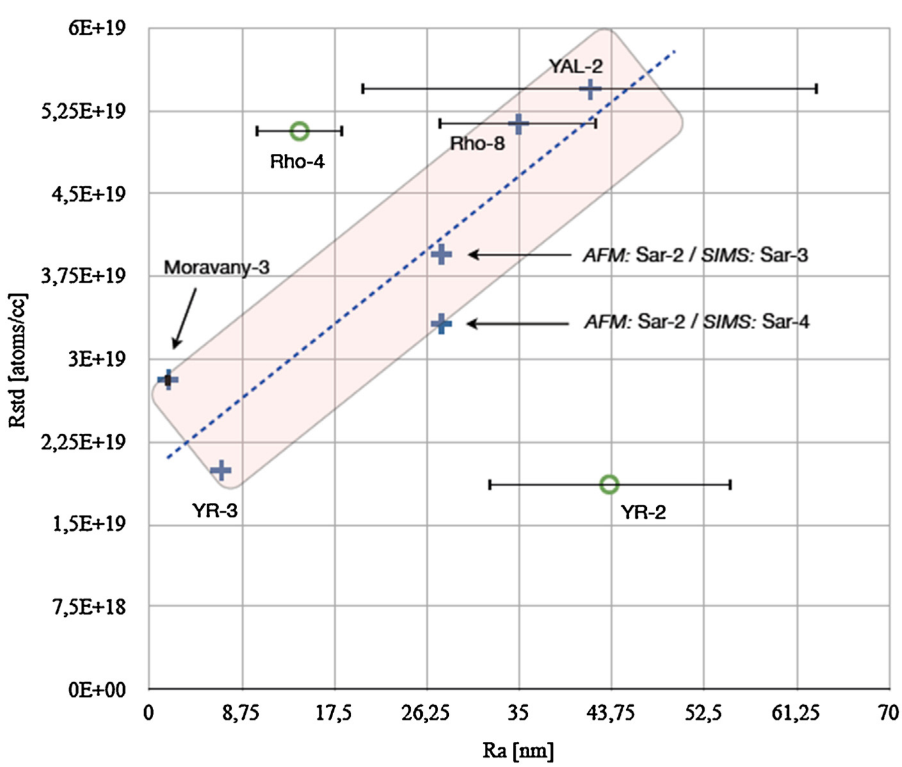

Fig. 7. Rstd coefficient versus R_a for eight pairs of AFM-SIMS measurements. AFM analysis of the five samples of the present work (YR-2, YAL-2, RHO-4, RHO-8, MORAVANY-3) and for sample YR-3 has been made in the same raster area investigated by SIMS. In the case of Sar-2, Sar-3 and Sar-4 samples AFM measurement has been made on Sar-2 and SIMS on samples Sar-3 and Sar-4 (The Sar-2,3,4 all derive from the Sarakinos Cave, Upper Paleolithic to Neolithic Settlement, Boeotia Prefecture, Greece; and have same provenance source from Melos island Aegean Sea).

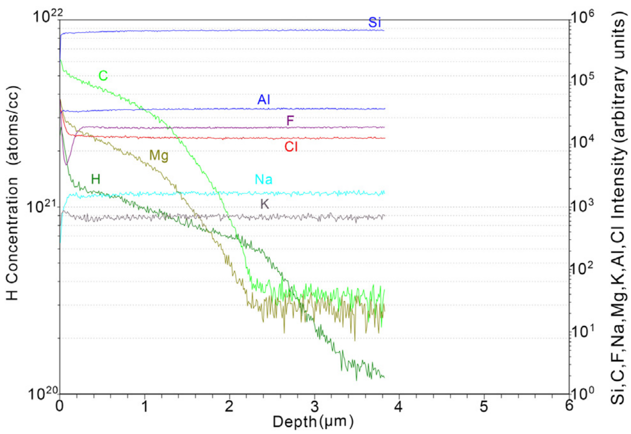

Fig. 9. Sar-7. H, Si, C, F, Na, Mg, K, Al and Cl profiles by Quadrupole SIMS.

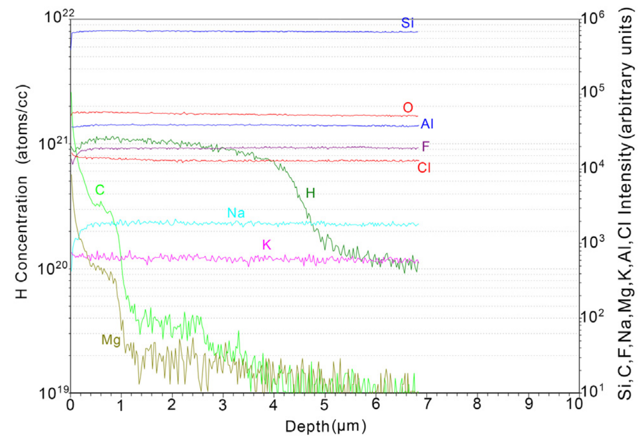

Fig. 10. Sar-8. H, Si, C, F, Na, Mg, K, Al and Cl profiles by Quadrupole SIMS.

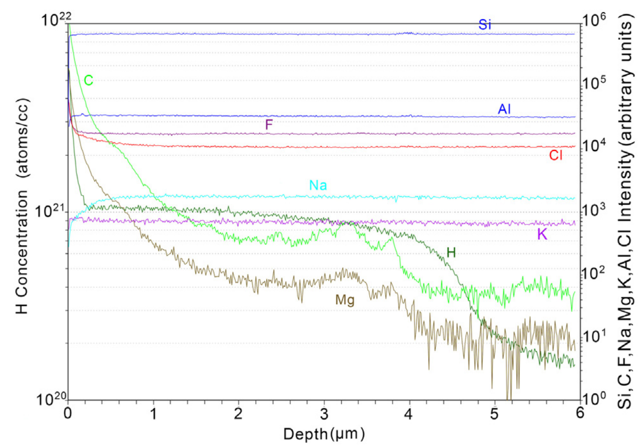

Fig. 11. As Fig. 10 (Sar-8) from different spot by Quadrupole SIMS.

in recent samples. Consequently, old samples need long ion bombardment times to reach the depth corresponding to the beginning of the hydrogen concentration profile. This produces an increase of the secondary roughness formed inside the crater and a higher dispersion of secondary ions, causing reduced accuracy in SIMS analyses.

The initial surface roughness affects the dispersion of secondary ions during sputtering that causes disturbed profiles of concentrations. Moreover, the roughness produced by the beam in the formed crater affects both the dispersion of secondary ions and the following accuracy of depth in the crater via the profilometer. The latter is due to the inhomogeneous structure of obsidian with cracks, voids and minerals spread over the obsidian body.

This internal “roughness” has been further supported by profiling of more cations of carbon, aluminium, fluorine, manganese, and getting 2D and 3D mapping of obsidians, all of which supplement the mentioned above findings, and provide an additional criterion for the suitability of H^+ SIMS profiles for SIMS-SS dating. Data have been produced with a quadrupole SIMS and by TOF-SIMS providing an insight to the structural status within the rind of the surface.

7. Depth profile with TOF-SIMS and Quad-SIMS

The impact on H^+ hydration profiles and/or of the hydration itself on the reported presence of carbon and nitrogen [23] in obsidian surfaces has been further investigated. This hypothesis was done by examining obsidian surfaces with Quad-SIMS and TOF-SIMS. Depth profiles of relative concentrations of carbon (C), along with fluorine (F), aluminum (Al) and magnesium (Mg), as well as, other cations are measured on some obsidian tools from archaeological sites in Aegean, Mainland Greece and Carpathian (Table 3).

Figs. 9–12 show the depth profiles of the afore mentioned elements for archaeological obsidians Sar-7, Sar-8, RHO-892 by quad-SIMS.

Carbon profiles relate that for Mg more than F and Al and both follow in general an exponential drop.

In all cases the disturbance of C—Mg was in the top surface layers (1–2 μm) but in sample Sar-8 (Fig. 11) the disturbance is in depth of approx. 3.5 μm. Such a disturbance in this depth is clearly evidence for a carbonate mineral microlithic (dolomite) inclusion. A leaching/enrichment is also observed in near surface for fluorine (Fig. 9a, b and Fig. 11), which may be due to the pH of immediate soil environment.

C and Mg exhibit a parallel exponential drop with similar disturbance at 0.8 μm. The inflection of H^+ curve coincides with the

Table 3
Samples, sites and SIMS measurements for cation profiles and mapping.

Sample code n°	Site	SIMS	Measurements
RHD-1024	Prophet Elias Hill Desfina (Delphi), Greece Surface find	TOF-SIMS	Surface composition (all) H profile up to 10 μm ^{16}O and ^{18}O profile
RHO-523	Moravany Early Neolithic Settlement, East Slovakia		Cations profile 3D mapping analysis (YR-3 and RHO-523)
YR-3	Cyclops Cave (late palaeolithic layer) Island of Youra, Alonissos, Greece [24]		
Sar-7 Sar-8 Sar-9	Sarakinos Cave, Upper Paleolithic up to Neolithic Settlement, Boeotia Prefecture, Greece [25]	Quadrupole SIMS	Profile of C, Mg, F, Al
RHO-892	Ikaria Island Mesolithic Settlement, Greece [26]		

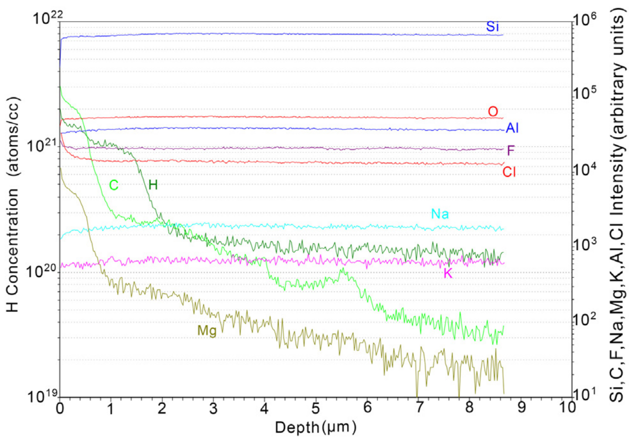

Fig. 12. RHO-892. H, Si, C, F, Na, Mg, K, Al, O and Cl profiles by Quadrupole SIMS.

pristine Mg and C in the obsidian, that is the Mg and C profiles follow the Fickian law of the first diffusion region, thereafter no further diffusion takes place (Fig. 9).

In spite the fact that Obsidian is a cryptocrystalline silica glass its microlithic inclusions that have crystalline lattices are dispersed in the amorphous body since its formation from lava. Such a structure has an impact in the hardness of the material. The presence of Mg in crystalline materials makes them more fragile and therefore at the time of cleaving (making a tool) pits or cavities may be formed in areas rich in Mg inclusions. The matching (same depth, width) between C and Mg disturbances in depth profiles show that (a) cavities or pits have a depth similar the width of the rich layer of Mg based inclusions, and (b) the existence of carbonate mineral inclusions. The commensurate variation in disturbances between C and Mg leads to a new criterion in measuring a H^+ depth profiles with SIMS; in all cases of measuring a depth profile in the hydration rim in obsidian, C and Mg must also be included in measurement.

Any disturbance in these profiles implies area with inclusions and the measurement must be redone in a different spot. Disturbance in Mg, F and Al profiles, implies this in H^+ profile too. Whereas H^+ profile is acceptable and the SIMS-SS age can be deduced, F and Al follow almost a straight line without disturbances and Mg follows an exponential curve. With problematic surface spots the F and Al no longer follow straight lines and Mg produces peaks along the exponential drop.

In the following two sections the above results are complemented by surface elemental mapping and 3D analysis as well as H^+ profile compared to cation in the rinds of obsidian tools.

8. Surface mapping and 3D analysis

Fig. 13 shows a surface map of a 103 × 103 μm area for several elements and Fig. 14 a X–Y slice with three color overlay of three compounds. The color scale is normalized to the brightest pixel.

Inspection of Figs. 13 and 14 the following remarks are drawn: (a) Hydrogen has uneven distribution over the surface with a maximum concentration in cracks and pits, (b) carbon and cyanide (CN^-) have the same distribution with hydrogen, which reveals the presence of micro-bacterial activity, (c) the main obsidian matrix contains ^{16}O with the distribution of ^{18}O to be much lesser, (d) fluorine is distributed over surface with maxima in cracks and pits, (e) sulfur and chlorine have increased concentration in spots of bacterial activity, (f) magnesium has decreased concentration in inclusions that have increased concentration in fluorine, and, (g)

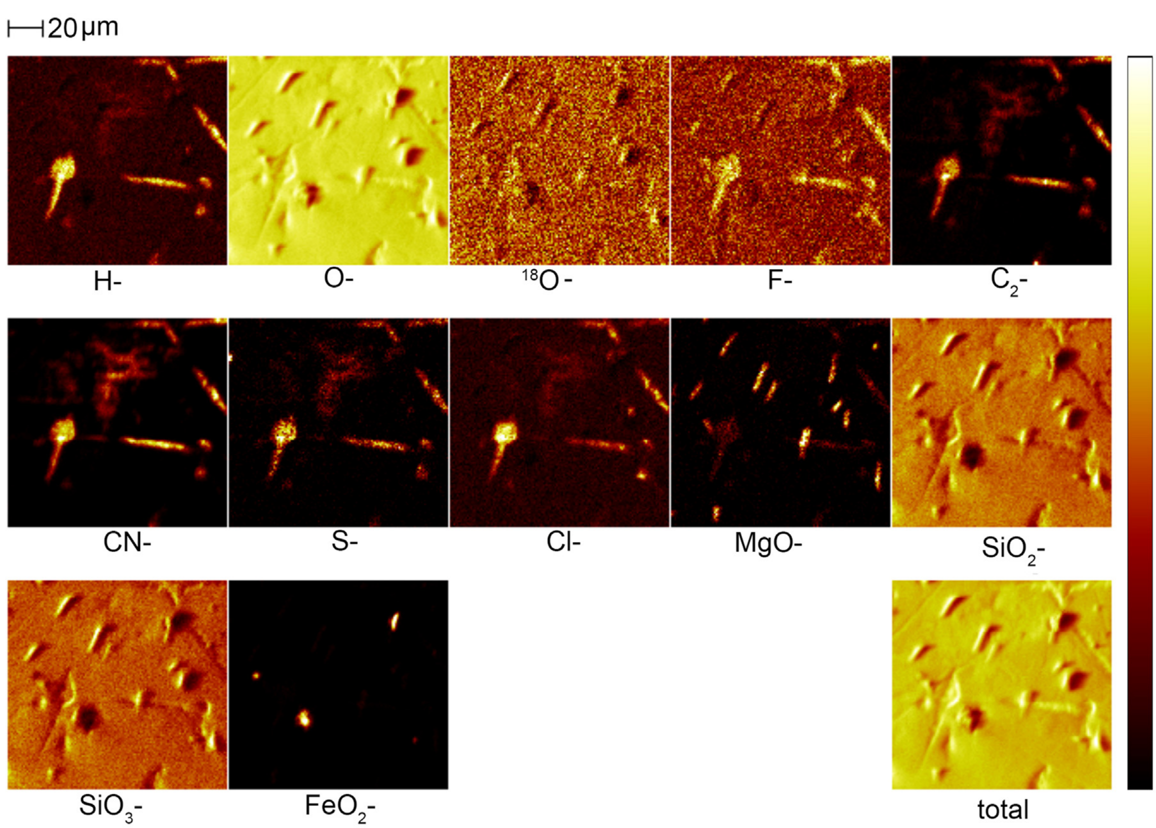

Fig. 13. 2D Surface mapping of Sample RHD-1024 by TOF-SIMS. 103 × 103 μm area. Distribution of H, ^{16}O, ^{18}O, F, MgO, CN, S, Cl, SiO_x, C, for sample RHO-1024. Scale refers in absent (black) to full homogeneous distribution of respective cation. Spots indicate crystallite and the left elongated bright spot rather a crack with increased hydrocarbons.

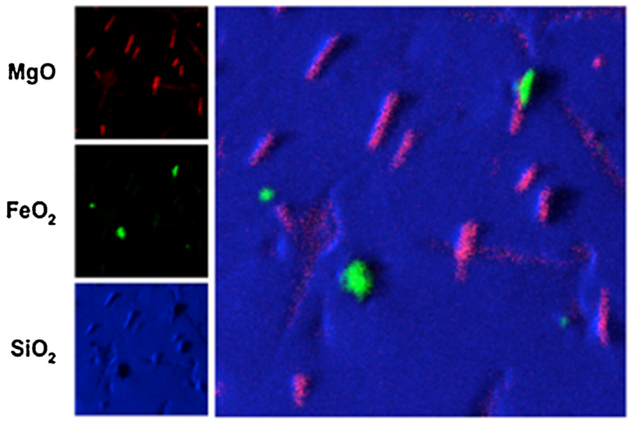

Fig. 14. Three color overlay for Fig. 13 for MgO, FeO_2, SiO_2, X–Y slice. Area ~100 × 100 μm.

the concentration of iron in spots with a shortage of silicon points the presence of Fe-inclusions.

Fig. 15 shows the 3D distribution of H, ^{16}O, ^{18}O, Cl, MgO, SiO_x for the same area as in Fig. 13. Inspection of Fig. 14 (second row) reveals that the formation of the hydration layer is uniform along X and Z axes. If the crater depth is about 4.2 μm, the hydration depth is 1.8–2 μm. The depth scale was calculated based on sputter rates determined on a suitable reference sample. Moreover, the increased H^+ concentration due to biological activity inside cracks may disturb the H^+ hydration profile giving higher values of hydrogen concentration, resulting to a disturbed of highly scattered SIMS H^+ profile. From the comparison of the second and the sixth image of Fig. 15 and Fig. 13 we conclude that ^{16}O and Silica decrease in areas of Fe-rich; ^{18}O seems to have a uniform distribution along depth, though beyond diffused layer both ^{18}O and ^{16}O exhibit a drop (Fig. 16b), areas rich in Mg are in deeper layers, while spots rich in Cl are limited to surface (see Figs. 6 and 10). Relevant mapping has been earlier used for characterization and provenance of ancient opaque glass [27].

9. Cation depth profiling

Figs. 16–18 demonstrate the depth profiles of H^+ in relation to other cations, for sample RHD-1024.

The different complementary techniques used were listed in Table 3. A depth scale was established by measuring the total crater depth of a suitable profile on RHD-1024 with a mechanical profiler and assuming linear sputter rates.

The depth of the point of inflection in the H^+ profile was used to establish depth scales for all other profiles acquired on RHO-1024. The accuracy of the depth scale is limited due to the strong surface roughness of the obsidian. The impact of surface roughness on SIMS measurements is in fact dealt with above; in addition, here, in Figs. 16–18 it is observed that the sigmoid shape of the hydrogen (hydration layer) is also found for the silicon hydroxyl (Si—OH). This strengthens the diffusion–reaction model suggested by late Doremus [4]. Also, it was found that none of the other element or compounds has any significant change except sodium. The near surface leaching of Na is due to trace element exchange with the burial environment.

10. Discussion

The roughness of obsidian surface and the detailed cation profiles and surface distribution in obsidians has been studied via AFM and SIMS and SIMS-TOF. The new data have been discussed per each section separately. Here we discuss other issues of cation profiles and the resulted interaction between obsidian surface and context with a due explanation related to leaching/enrichment.

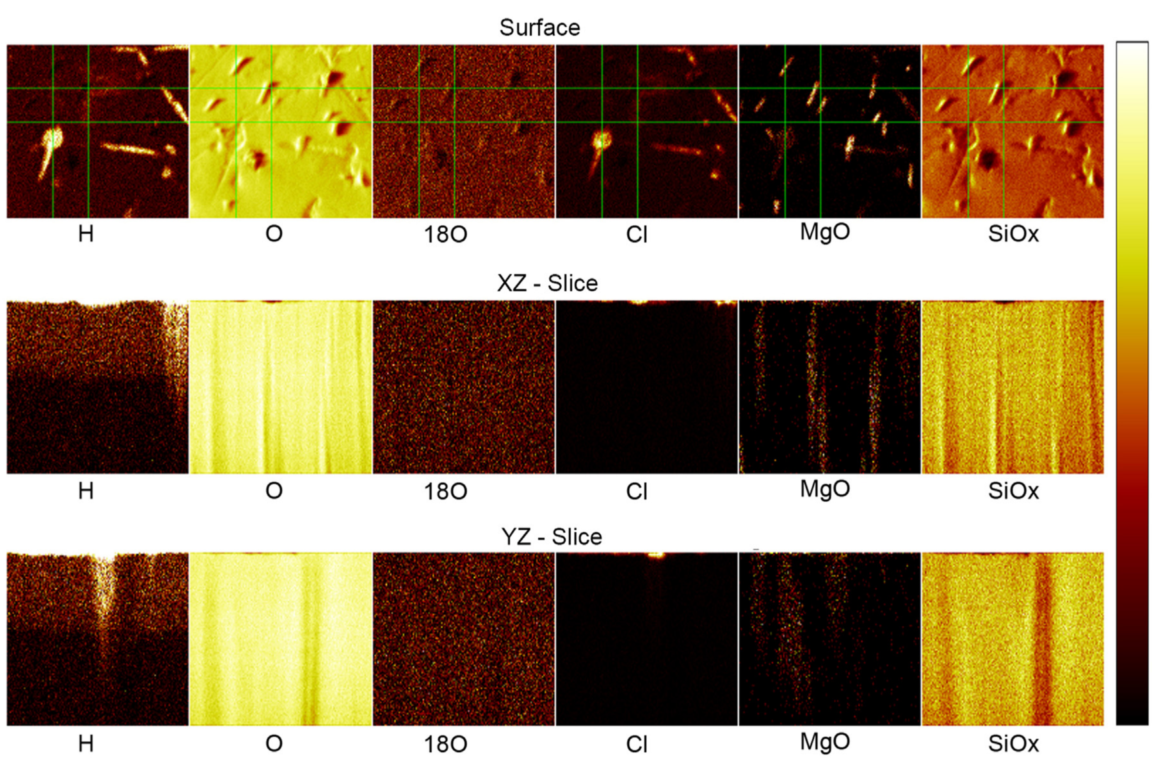

Fig. 15. 3D cross-sections by TOF-SIMS. Sample RHD-1024. Detail of Fig. 13. First row: X–Y distribution integrated over total sputtered depth. Second row: X–Z slices along green line, viewing direction from the bottom. Third row: Y–Z slices along green line, viewing direction from the left. Total crater depth 4.2 μm. Note in the middle left XZ row for H the boundary between diffused rim (upper) and non-diffused part, as well as, a vertical crack apparent in YZ.

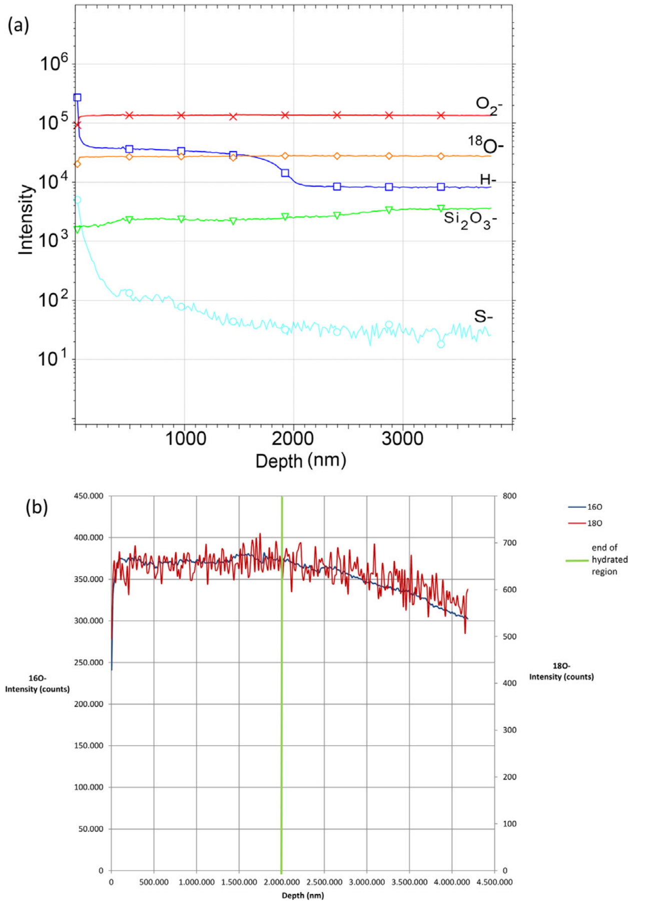

Fig. 16. (a) H^+ profile RHO-1024 in logarithmic scale by TOF-SIMS, (b) ^{16}O, ^{18}O versus depth in linear scale.

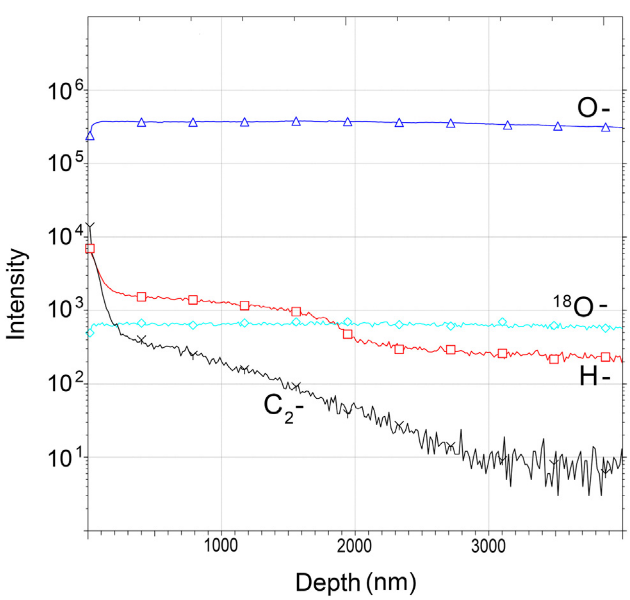

Fig. 17. H, C, ^{16}O and ^{18}O profiles in logarithmic scale for RHO-1024 by TOF-SIMS.

The H^+ was studied intentionally because the main purpose was the SIMS-SS dating method (explained in the introduction and abstract too). Isotopes of ^{18}O and the Si—OH have been also recorded. The former, and ^{16}O as well, seem constant, but in linear scale both drop slightly per depth, though of similar trend; while the latter follows H^+ trend. Si—OH implies dissolution during

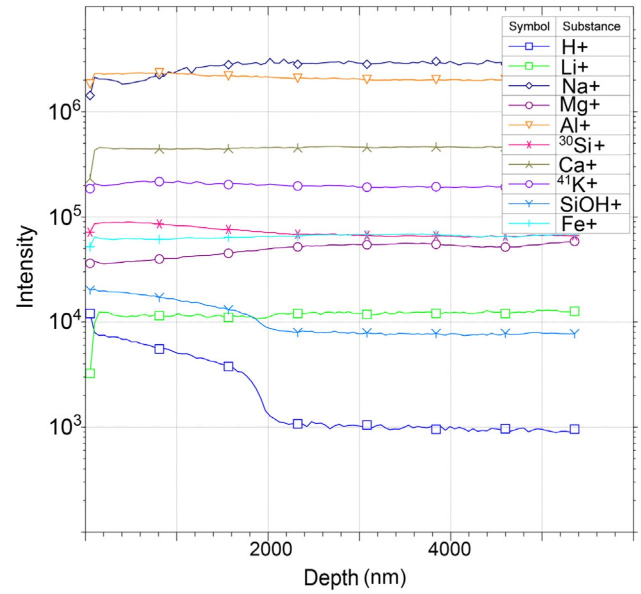

Fig. 18. Depth distribution of cations in logarithmic scale for RHO-1024 by TOF-SIMS.

diffusion of water transport in a reaction manner similar to the produced H^+.

Cations Ca, Si, Al, Li, Na have been discussed in earlier works ([28,29]). Indeed, leaching of cations from the glass or enrichment from the surrounding is possible. This depends upon the ion exchange and network dissolution reactions which in turn is a function of pH, temperature and chemistry of surrounding context, as well as, the chemical composition, pristine (structural) water and crystalline presence in obsidians. Such exchange diffusion–reaction phenomena are variable on how they have therefore progressed into the glass and at what (different?) rates over time. For example, sample 1024, collected as surface find, shows progressive Na leaching that is coupled with dissolution of the silicate matrix in the outermost 2 μm after at least 6000 years of burial.

No reaction and ion exchange is observed for K, ^{18}O, Al. Slight enrichment for sulphur to the depth of 1.5 μm, and slight leaching occurs for Si_2O_3 (gradual leaching to 3.5 μm) implying outward diffusion process, Li (slight leaching to 0.2 μm), Ca (slight leaching at a depth of 0.2 μm).

In an earlier work by SEM-EDAX scanning a surface scrap of a semi-finished blade at Ftelia Neolithic settlement Mykonos island Greece the leaching of Si, K, Na and some Fe on the surface is observed. Enrichment of Ca and Al is present. On a preliminary examination, in flakes with the widest weathered zone, enrichment of Ti, Fe, Mg and Al was detected on the surface, while Si, Na and K have been leached out. On tools, the enrichment is not as obvious as the leaching of Si, Na and K. The apparent difference between tools and flakes is due to age (archaeological versus geological) differences [29].

Following up the SIMS analysis, AFM were performed in same raster area and the obtained ages were: Yr-3, 8140 ± 1350; RHO-4, 6620 ± 350; YR-2, 9370 ± 516. Although these ages obtained follow criteria above the RHO-4 and YR-2 deviated from the linear tend of Fig. 7 due to different examined area. This issue resets the concern in choosing strictly appropriate area for SIMS and AFM for age calculation [30].

It is prudent to present the steps involved in the dynamic reaction of hydrolysis at the initial surface layers. In such a dynamic environment the formation of silanol groups, the cation exchange due to water diffusion into the obsidian body but the hydrolysates from soil, the leaching gradients of different species, and the isotopic $^{16}O/^{18}O$ gradual drop deeper that the diffused area, are considered to be due to the following four mechanisms during the obsidian exposed to water and soil solution during burial time [31].

First, the glass surface responds to the stress of a fracture by becoming reactive enough to "sorb" a variety of molecules; Second, dissociated molecules from the fluid phase diffuse inside the fresh obsidian through a mesoscopic network of fractures. H_3O^+ ions exchange at a very high rate (the "initial rate") (see, Fig. 6a), with available network modifiers that are water soluble, such as alkalis (but also alkaline-earths and divalent transition elements). This so-called "inter-diffusion" effect is initially intense but quickly reaches a steady state with time except possibly in closed systems after long exposures that forms the surface saturation layer (SS) a crucial parameter in SIMS-SS dating method [32] (see section 5.2 above). In a closed system, the pH will locally increase at the interface because of the formation of silanol groups (Si—OH) and the leaching of "free" aqueous ions that were formerly network modifiers; the third step is characterized by hydrolysis of the network-formers of the tetrahedral framework of the obsidian glass structure, in competition with the previous stage. The formation of these hydrous silica species corresponds to a quasi-congruent dissolution of the glass. Until the leached species concentrations reach aqueous saturation levels, the glass dissolution rate will decrease as much as the silica concentration in the solution increases. When saturation is reached (SS layer Fig. 6A and section 5.2), the fourth step begins and it involves surface precipitation of hydrolyzed elements that are less soluble (e.g. Si(IV), Al(III), Fe(III), Ti(IV), REE's, and others) that are encountered in many soils resulting from intense tropical weathering (laterites) of primary endogenous rocks. During this stage, a gel phase is formed at the obsidian/water interface, which is highly hydrous and thus highly sensitive to dehydration. Within soils, the gel will be exposed to concentration and redox gradients and temporal perturbations (among others) [33]. Non steady state conditions will strongly affect these processes, particularly cyclic episodes (such as those produced by seasonal variations), which will induce the formation of layers at the glass surface. This evolution suggests that these steps are not well separated in time: they all occur continuously.

Concerning the $^{16}O/^{18}O$ variation (Fig. 16b) along the diffused layer of 2 μm we observe a change around an average value within $\pm$ 10%, and a slight drop in deeper layers by 20% in 2 microns. It is not clear at this stage the causes of this, and we suggest the former might reflect palaeotemperatures during the archaeological period and the average is the effective hydration temperature sought in OHD dating to estimate diffusion coefficient from Arrhenius plots [34]; and the former a fractionation effect due to temperature gradient of magma cooling in surface. Another possible explanation is an isobaric interference, that this signal at $m/z = 18$ is related to hydration and it is probably coming from $H^{17}O^+$ isotope or from $H_2{}^{16}O^+$ signal. More work will clarify this.

11. Conclusion

New results highlight a linear correlation between the dispersion of the concentration values in the hydration profiles determined by SIMS and the surface roughness obtained through AFM. Roughness ranges from some 3 nm up to 100 nm, together with cation profiling monitoring, are both of crucial importance as they introduce a solid criterion for assessing the reliability of SIMS analyses of obsidians, given that roughness represents a critical aspect when dating archaeological glasses. In this framework, the roughness experimental data obtained by AFM are extremely valuable, as they are not affected by the same effect of SIMS profiles, and they can therefore be used to have a prior validation of SIMS data for dating. Concluding, the results presented in this paper further confirm the criterion we previously introduced relying on the AFM analysis of the surface of obsidians prior to SIMS investigation.

The obsidian surface 2D and 3D mapping and cation along the rind with quad-SIMS and ToF-SIMS explains the increased scatter of SIMS H^+ profiles for obsidian SIMS-SS dating. The mapping of the surface with ToF-SIMS prior to depth profile can be used to locate areas free of cracks, pits, troughs, shoulders or inclusions ensuring a depth profile of high accuracy. Measuring of hydration profile along with other elements (fluorine, magnesium, carbon) provided useful information for the reliability of the SIMS H^+ profile measurement, as well as, clues regarding ion exchange reactions and the environmental context leading to leaching or enrichment that alter surficial dynamic layers in the scale of few micrometers, that is in the rim, and all are useful data for OHD. In fact depth profiles of relative concentrations of carbon (C), along with fluorine (F), aluminum (Al) and magnesium (Mg), as well as, other cations measured on obsidian tools from archaeological sites indicated either leaching or enrichment, a distorted profile of constant or similar trend to H^+ profile. The commensurate variation in disturbances between C and Mg indicates that in measuring a H^+ depth profile in the hydration rim in obsidian, C and Mg must also be included in measurement and compared to H^+. The 2D surface mapping by TOF-SIMS indicated crystallites and cracks with increased hydrocarbons.

It is of interest that the S-like trend of the hydrogen (hydration layer) is also found for the silicon hydroxyl (Si—OH) which reinforces the diffusion–reaction model. The near surface leaching of Na is due to trace element exchange with the burial environment.

Acknowledgements

N.L. and I.L. thank the director of NCSR "Demokritos" and the staff for helping N.L. with the AFM measurements, Dr. Steven Novak (University at Albany, USA) for quad-SIMS measurements and useful comments, Dr. Markus Terhorst of the ION-TOF for the financial support of the ToF-SIMS measurements. M.B. and F.R. thank CSGI and MIUR-PRIN 2010 for financial support. M.B. thanks the EU for the financial support (FP7-PEOPLE-2009-RG, Project: SUPRACRYST). Ioannis Liritzis and Fahad Mutlaq Al-Otaibi extend their appreciation to the Deanship of Scientific Research at King Saud University for funding the work through the research group project No. RGP-VPP-194.

References

[1] T. Drury, G. Roberts, Diffusion of water in silica Glass, Plenum Press, New York, 1962, pp. 249–255.
[2] W. Lanford, Glass hydration: a method of dating glass objects, Science 196 (1977) 975–976.
[3] M. Nogami, M. Tomozawa, Diffusion of water in high silica glasses at low temperature, Phys. Chem. Glasses 25 (1984) 82–85.
[4] R. Doremus, Diffusion of water in rhyolite Glass: diffusion-reaction model, J. Noncrystalline Solids 261 (2000) 101–107.
[5] I. Liritzis, Obsidian hydration dating, in: W.J. Rink, J.W. Thompson (Eds.), Encyclopedia of scientific dating methods, Springer-Verlag, Berlin-Heidelberg, 2014, pp. 1–23, http://dx.doi.org/10.1007/978-94-007-6326-5_39-1.
[6] I. Liritzis, N. Laskaris, The SIMS obsidian hydration dating method (Ch. 3), in: The dating and provenance of obsidian and ancient manufactured glasses, New Mexico Press, 2012, pp. 26–45.
[7] I. Liritzis, N. Laskaris, Fifty years of obsidian hydration dating in archaeology, J. Noncrystalline Solids 357 (2011) 2011–2023.
[8] I. Liritzis, M. Bonini, N. Laskaris, Obsidian hydration dating by SIMS-SS: surface suitability criteria from atomic force microscopy, Surf. Interface Anal. 40 (2008) 458–463.
[9] I. Liritzis, N. Laskaris, M. Bonini, Nano- and micro- scale resolution in ancient obsidian artefact surfaces: the impact of AFM on the obsidian hydration dating by SIMS-SS, Physica Status Solidi C 5 (2008) 3704–3707.
[10] G. Binnig, C.F. Quate, C. Gerber, Atomic Force Microscope, Phys. Rev. Lett. 6 (9) (1986) 930–933.
[11] I. Schmitz, T. Prohaska, G. Friedbacher, M. Schreiner, M. Grasserbauer, Investigation of corrosion processes on cleavage edges of potash-lime-silica glasses by atomic force miscroscopy, Anal. Bioanal. Chem. 353 (5–8) (1995) 666–669.

[12] M. Schreiner, G. Woisetschlager, L. Schmitz, M. Wadsak, Characterisation of surface layers formed under natural enviromental conditions on medieval stained 277 glass and copper alloys using SEM, SIMS and atomicforce microscopy, J. Anal. Atomic Spectrosc. 14 (1999) 395–403.
[13] N. Carmona, A. Kowal, J. Rincon, M. Villegas, AFM assessment of the surface nano/microstructure on chemical damaged historical and model glasses, Mater. Chem. Phys. 119 (2010) 254–260.
[14] N. Zacharias, G. Mastrotheodoros, M. Katsiotis, N. Laskaris, Glazedpottery surfaces under the microscope: which criteria to decide about archaeological and modern items, in: 38th International Symposium on Archaeometry, Tampa, Florida, 2010.
[15] M. Melcher, R. Wiesinger, M. Schreiner, Degradation of glass artifacts: application of modern surface analytical techniques, Acc. Chem. Res. 43 (6) (2010) 916–926.
[16] S. Novak, C. Stevenson, Aspects of SIMS depth profiling for obsidian hydration dating, the dating and provenance of obsidian and ancient manufactured glasses (Ch. 1), New Mexico Press, 2012.
[17] A. Benninghoven, F. Rudenauer, H. Werner, Secondary ion mass spectrometry: basic concepts, instrumental aspects, applications and trends, New York, J. Willey and Sons, 1987.
[18] D. McPhail, M. Dowsett, Dynamic SIMS, in: Surface analysis – the principal techniques, 2nd ed., John Wiley and Sons Ltd, 2009.
[19] F. Stevie, P. Kahora, D. Simons, P. Chi, Secondary ion yield changes in Si and gas as due to topography changes during O2 or Cs+ ion bombardment, J. Vaccum Sci. Technol. (1988) 76–80.
[20] P.V.D. Heide, M. Lim, S. Pery, J. Bennett, A systematic study of thesurface roughening and sputter rate variations occurring during SIMS ultra shallow depth profile analysis of Si with Cs+, Nucl. Instrum. Methods Phys. Res. B 201 (2003) 413425.
[21] B. Fares, C. Dubois, B. Gautier, J. Dupuy, F. Cayrel, G. Gaudin, Afmstudy of the SIMS beam induced roughness in monocrystalline silicon in presence of initial surface or bulk defects of nanometric size, Appl. Surf. Sci. 252 (2006) 6448–6451.
[22] K. Wittmaack, Towards the ultimate limits of depth resolution in sputter profiling: beam induced chemical changes and the importance of sample quality, Surf. Interface Anal. 21 (1994) 323–335.
[23] S. Patel, R. hedges, J. Kilner, Surface analysis of archaeological obsidian by SIMS, J. Archaeol. Sci. 25 (1998) 1047–1054.
[24] A. Sampson, The cave of the Cyclops. Mesolithic and Neolithic networks in the northern Aegean, Greece, Vol. II, INSTAP Academic Press, Philadelphia, Pennsylvania, 2011.
[25] A. Sampson, The Neolithic and the Bronze Age, The Sarakenos Cave of Akraephnion, Boeotia, Greece. Vol. I, University of the Aegean and Polish Academy of Arts and Sciences, Athens, 2008.
[26] I. Liritzis, N. Laskaris, Obsidian hydration dating from hydrogen profile using SIMS: applications to Ikarian specimens, Folia Quaternaria 80 (2012) 45–54.
[27] F.J.M. Rutten, D. Briggs, J. Henderson, M.J. Roe, The application of time-of-flight secondary ion mass spectrometry (TOF-SIMS) to the characterization of opaque ancient glasses, Archaeometry 51 (6) (2009) 966–986.
[28] S.D. McLoughlin, R.J. Hand, N.C. Hyatt, W.E. Lee, I. Notingher, D.S. McPhail, et al., The long term corrosion of glasses: analytical results after 32 years of burial at Ballidon, Glass Technol. Eur. J. Glass Sci. Technol. A 47 (3) (2005) 59–67.
[29] I. Liritzis, M. Diakostamatiou, C.M. Stevenson, S.W. Novak, J. Abdelrehim, The dating of hydrated obsidian surfaces by SIMS-SS, J. Radioanal. Nucl. Chem. 261 (1) (2004) 51–60.
[30] I. Liritzis, N. Laskaris, Advances in obsidian hydration dating by secondary ion mass spectrometry: world examples, Nucl. Instr. Methods Phys. Res. B 267 (2009) 144–150.
[31] F. Farges, M.-P. Etcheverry, A. Haddi, P. Trocellier, E. Curti, G.E. Brown, Durability of silicate glasses: an historical approach SLAC-PUB-12221, in: Contributed to 13th International Conference on x-ray absorption fine structure (XAFS13), July 9-14, 2006, Stanford, California, 2006.
[32] I. Liritzis, SIMS-SS A new obsidian hydration dating method: analysis and theoretical principles, Archaeometry 48 (3) (2006) 533–547.
[33] P. Aagard, H.C. Helgeson, Thermodynamic and kinetic constraints on reaction rates among minerals and aqueous solutions: I. Theoretical considerations, Am. J. Sci. 282 (1982) 237–285.
[34] A.T. Rogers, Field data validation of an algorithm for computing obsidian effective hydration temperature, J. Archaeol. Sci. 35 (2) (2008) 441–447, http://dx.doi.org/10.1016/j.jas.2007.04.009.